Biochimie 113 (2015) 125–133

Contents lists available at ScienceDirect

Biochimie

journal homepage: www.elsevier.com/locate/biochi

Research paper

Understanding the stability of DNA G-quadruplex units in long human telomeric strands

Anthony Bugaut [a, b, c], Patrizia Alberti [a, b, c, *]

[a] Muséum National d'Histoire Naturelle, Sorbonne Universités, 57 rue Cuvier, CP 26, 75005 Paris, France
[b] CNRS UMR 7196, 57 rue Cuvier, CP 26, 75005 Paris, France
[c] Inserm U 1154, 57 rue Cuvier, CP 26, 75005 Paris, France

ARTICLE INFO

Article history:
Received 20 February 2015
Accepted 3 April 2015
Available online 14 April 2015

Keywords:
G-quadruplexes
Contiguous G4
Tandem G4
Stability
Telomeres

ABSTRACT

Human telomeric DNA is composed of GGGTTA repeats. The presence of consecutive guanines makes the telomeric G-strand prone to fold into contiguous (or tandem) G-quadruplexes (G4s). The aim of this study was to provide a clarified picture of the stability of telomeric tandem G4 structures as a function of the number of G4 units and of boundary sequences, and an understanding of the diversity of their melting behaviors in terms of the single G4 units composing them. To this purpose we undertook an UV-spectroscopic investigation of the structure and stability of telomeric repeats potentially able to fold into up to four contiguous G4s, flanked or not by TTA sequences at their 5′ and 3′ extremities. We explain why the stability of $(GGGTTA)_{4m-1}GGG$ structures ($m = 2, 3, 4 \ldots$) decreases with increasing the number m of G4 units, whereas the stability of TTA-$(GGGTTA)_{4m-1}$GGG-TTA structures does not. Our results support that the inner G4 units have similar stabilities, whereas the stabilities of the terminal G4 units are modulated by their flanking nucleotides: in a TTA-$(GGGTTA)_{4m-1}$GGG-TTA tandem context, the terminal G4 units are roughly as stable as the inner G4 units; while in a $(GGGTTA)_{4m-1}GGG$ tandem context, the G4 at the 5′ extremity is more stable than the G4 at the 3′ extremity, which in turn is more stable than an inner G4. Our study provides new information about the global and local stability of telomeric tandem G4 structures under near physiological conditions.

1. Introduction

Telomeres are nucleoprotein complexes that cap the extremities of eukaryotic linear chromosomes. They ensure genome stability by providing a solution to the end-replication problem and to the end-protection problem [1,2]. In most eukaryotes, telomeric DNA is composed of tandem repeats of a short motif bearing consecutive guanines running from 5′ to 3′ [3], and ends with a single-stranded 3′-overhang. The presence of clusters of guanines makes the telomeric G-rich strand and, in particular, the 3′ single-stranded overhang prone to fold into G-quadruplexes [4]. G-quadruplexes (or G4s) are a family of four-stranded structures resulting from the formation and stacking of tetrads of hydrogen-bonded guanines and stabilized by several cations, notably by the physiological relevant cations sodium and potassium.

Several cellular studies indicate that G4s may form at telomeres. In hypotrichous ciliates, telomeric 3′-overhangs form G4s that link together the gene-sized chromosomes of the macronucleus (for review [5]). In budding yeasts, G4s appear to be involved in telomere capping, at least when natural capping is impaired [6]. In mammalian cells, indirect evidence suggests that G4s may occur at telomeres during replication and at the 3′-overhangs, challenging telomere maintenance, at least in the absence of proteins able to unfold G4s or in the presence of ligands able to stabilize these structures [7–10]. Telomeric G4s modulate *in vitro* telomerase activity [11–13] and binding of other proteins involved in telomere biology, as recently demonstrated by single-molecule approaches [14,15].

It is well established that four repeats of the human telomeric motif GGGTTA fold, *in vitro*, into a variety of G4 conformations [16–23]. Nevertheless, the high number of GGGTTA repeats makes the human telomeric G-strand potentially apt to fold into contiguous (or tandem) G4s, formed by the 21mer sequence $(GGGTTA)_3GGG$ and connected by TTA linkers, in particular at the 3′-overhangs (200 nucleotide average length [24,25]). Contiguous G4s

* Corresponding author. Muséum National d'Histoire Naturelle, 57 rue Cuvier, CP 26, 75005 Paris, France.
E-mail address: alberti@mnhn.fr (P. Alberti).

http://dx.doi.org/10.1016/j.biochi.2015.04.003

are attractive structures for the design of telomere specific small ligands, with the ability to discriminate between isolated single G4s and contiguous G4s [26,27]. Do long telomeric strands actually fold into contiguous G4s? And how stable these structures are?

An early study from Yu et al. on $(TTAGGG)_{n=4-12}$ sequences suggested that structures formed by eight and twelve repeats are more ordered than the others and a model of non-interacting contiguous G4s was proposed [28]. Formation of a higher-order architecture consistent with contiguous G4s was then revealed by atomic force microscopy [29]. A later *in vitro* study brought additional evidence of folding into two and three contiguous G4s [30]. Recently, structural investigations by nuclear magnetic resonance of individually labeled G4 units provided some insights into the conformations of the different G4 units in a tandem context [31,32].

To date only a few studies provided some data about the global stability of structures formed by long telomeric strands. Vorlickova et al. reported that the thermal stability of the structures formed by $(GGGTTA)_{n=1-16}GGG$ sequences depends on the number of repeats [33]. Nevertheless, the authors did not provide evidence of folding into contiguous G4s, hence it is not clear if the decrease in stability upon increasing the number of potential G4 units results from irregular folding of long telomeric strands or from other reasons. Bauer et al. reported that $(GGGTTA)_{7,11}GGG$ structures display the same thermal stability and fold, each, into more than one conformers; they argued that the end of telomeres can form only a few tandem G4s (fewer than three) [34]. Petraccone et al. reported that $(TTAGGG)_{8,12}$ and $(TTAGGG)_{8,12}TT$ sequences fold into two and three contiguous G4s and that the global structures display identical melting temperatures and complex melting behaviors; they suggested that the G4 units are not identical nor independent and that unfavorable interactions of an unknown nature could limit complete folding of the telomeric overhang into contiguous G4s [30].

Overall, the published data do not yet allow drawing a clear picture of the stability of structures formed by sequences mimicking the telomeric 3′-overhang and, moreover, no study has provided an understanding of the observed melting behaviors. Major questions are still open. Does the global stability of these structures depend on the number of G4 units? If yes, why? Do the G4 units interact between them? Does the stability of a G4 unit depend on its position along the tandem structure? Answering to these questions will provide information about the possibility of folding of the telomeric 3′-overhang into contiguous G4s and about the global and local stability of these higher-order structures.

In this work, we present a systematic study aiming at the comprehension of the stability of telomeric tandem G4 structures. We carried out an UV-spectroscopic investigation of the structures and stabilities of telomeric repeats potentially able to fold into up to four contiguous G4s, flanked or not by TTA sequences at their 5′ and 3′ extremities. Besides extending the characterization of telomeric sequences to four potential G4 units, our study brings an original contribution to the comprehension of the stability of tandem G4 structures formed by long telomeric strands. Our work allows explaining their stability as a function of the number of G4 units and of boundary sequences in terms of the single G4 units composing them. Our work provides a framework to interpret the apparent diversity and complexity of melting behaviors of structures formed by long telomeric sequences in terms of the single G4 units composing them.

2. Material and methods

2.1. Oligonucleotides

PAGE purified oligonucleotides (H21, H45, H69, H93, H51, H75 and H99) and Reverse-Phase Cartridge•Gold™ purified oligonucleotides (H21-TTA, TTA-H21-TTA, TTA-H21, TTA-H45, H45-TTA, H21-$(TTA)_2$-H21 and H21-$(TTA)_3$-H21) were purchased from Eurogentec (Belgium), dissolved in bi-distilled water at a concentration of 200 μM and stored at −20 °C. Concentrations were determined by ultraviolet absorption in bi-distilled water, using molar extinction coefficients provided by the manufacturer.

2.2. Spectroscopic measurements

Oligonucleotide samples were prepared in a 10 mM cacodylic acid buffer at pH 7.2 (adjusted with LiOH), containing 100 mM NaCl or KCl. Ultraviolet (UV) absorption spectra and UV absorption measurements as a function of temperature were recorded on an Uvikon XL spectrophotometer (Secomam), equipped with a circulating water bath (Julabo) and with a dry airflow in the sample compartment. For melting profiles, samples were heated at 95 °C for 2 min, cooled at 5 °C, kept at 5 °C for 1 h, heated at 95 °C and cooled again at 5 °C, at a rate of 0.2 °C min^{-1}; the absorbance was recorded at 245, 260, 273, 295 and 335 nm, every 5 min. Temperature was measured with a glass sensor immersed into a water filled quartz cell. Melting profiles were corrected by subtracting the absorbance at 335 nm as a function of temperature. Thermal difference spectra (TDS) [35] were obtained by subtracting the absorbance spectrum at 5 °C (after annealing at 0.2 °C min^{-1}) from the one at 95 °C. Circular dichroism (CD) spectra were recorded on a J-810 spectropolarimeter (Jasco), at 5 °C, after annealing at 0.2 °C min^{-1}. Each CD spectrum was obtained by averaging three scans at a speed of 500 nm min^{-1} and was corrected by subtracting the spectrum of a solvent filled quartz cell. All measurements were carried out in quartz cells (Hellma) with an optical pathway of 1 cm; a layer of mineral oil prevented solution evaporation. Each melting experiment was performed at least twice, melting profiles and melting temperature values were reproducible.

2.3. Analysis of thermal melting curves

Melting curves were analyzed as described by Mergny and Lacroix [36]. Melting temperatures (T_m) were graphically determined as the intercept between the melting curves and the median lines of low-temperature and high-temperature absorbance linear baselines. Melting transitions of the single G4s formed by H21-TTA, TTA-H21-TTA and H21-TTA oligonucleotides were analyzed according to a two-state model, assuming ΔH^0 and ΔS^0 independent of temperature. The oligonucleotide folded fraction f was determined by the melting profile, normalized between 0 and 1, assuming linear low- and high-temperature absorbance baselines. The enthalpy and entropy changes upon folding, ΔH^0 and ΔS^0, were determined by a linear fit of Ln K_f vs $-1/T$ (where $K_f = f/(1-f)$ and T is the absolute temperature) according to the van't Hoff equation $\text{Ln}\, K_f = -\Delta H^0/RT + \Delta S^0/R$ (where R is the ideal gas constant), in the temperature range corresponding to $0.10 < f < 0.90$. The Gibbs free energy change upon folding, $\Delta G^0(T)$, was determined by the equation $\Delta G^0(T) = \Delta H^0 - T\Delta S^0$. For these three sequences, fitting according to a two-state model was satisfactory (the correlation coefficients for linear fits of Ln K_f vs $-1/T$ were greater than 0.99).

2.4. Polyacrylamide gel electrophoresis

Oligonucleotide samples were prepared in a 10 mM cacodylic acid buffer at pH 7.2 (adjusted with LiOH), containing 100 mM NaCl or KCl, at strand concentrations corresponding to 60 μM of potential G4 units (60 μM of H21, 30 μM of H45 and H51, 20 μM of H69 and H75, 15 μM of H93 and H99). Samples were heated at 90 °C for 2 min and slowly cooled at 4 °C, supplemented with sucrose (10%), and loaded (10 μl) into a 16.5 cm × 14.5 cm × 0.1 cm 12%

polyacrylamide gel (acrylamide:bisacrylamide 19:1) prepared in a TBE buffer containing 20 mM NaCl or KCl. Electrophoresis was run in a cold room at 4 °C, for 2 h and 30 min, at 3 W per gel, in a TBE buffer supplemented with 20 mM NaCl or KCl. The temperature of the gel, during electrophoresis, was about 15 °C. Oligonucleotides were detected by UV-shadow at 254 nm with a G:BOX (Syngene).

3. Results

3.1. Formation and stability of contiguous G4s by $(GGGTTA)_{7,11,15}GGG$ sequences

We first investigated the behavior of $(GGGTTA)_{3,7,11,15}GGG$ sequences (named H21, H45, H69 and H93, respectively), potentially able to fold into one, two, three and four contiguous G4s, respectively (Table 1). To date, spectroscopic evidence of folding of telomeric strands into up to four contiguous G4s has not yet been reported. In order to ascertain folding into contiguous G4s, we compared thermal difference spectra (TDS) [35] and circular dichroism (CD) spectra of the different oligonucleotides. We worked in a 100 mM KCl buffer, at the following strand concentrations: 6 μM for H21, 3 μM for H45, 2 μM for H69 and 1.5 μM for H93. These concentrations correspond to an identical concentration (6 μM) of potential G4 units for each oligonucleotide. We recorded CD spectra and low temperature absorption spectra for TDS at 5 °C; at this temperature H21 is completely structured. Under these conditions, H21, H45, H69 and H93 displayed TDS and CD spectra of very similar shapes and amplitudes (Fig. 1A and B). Since for a given oligonucleotide structure, the amplitudes of TDS and CD spectra are proportional to the concentration of the structure, this result supports that the concentrations of G4 units in H45, H69 and H93 samples are identical to the one of H21 (6 μM). In other words, this means that H45 folds into two G4 units per strand (6 μM of G4 units/3 μM of H45 strand), H69 folds into three G4 units per strand (6 μM of G4 units/2 μM of H69 strand) and H93 folds into four G4 units per strand (6 μM of G4 units/1.5 μM of H93 strand). In a non-denaturing polyacrylamide gel electrophoresis (PAGE) experiment, each of the three oligonucleotides H45, H69 and H93 migrated as a well-defined single band (Fig. 2); this further supports folding of each oligonucleotide into a single stable conformer.

Once established that $(GGGTTA)_{7,11,15}GGG$ (i.e. H45, H69 and H93) fold into two, three and four contiguous G4, respectively, we wondered why their thermal stability decreases upon increasing the number of G4 units (68, 59, 56 and 54 °C for H21, H45, H69 and H93, respectively) (Fig. 1C). H69 and H93 tandem structures clearly display complex melting profiles (the first derivative of their absorbance with respect to temperature has a peak at 61 °C and a shoulder around 40 °C), suggesting that they may be composed of G4 units of different stabilities. When representing the G4 structures formed by $(GGGTTA)_{3,7,11,15}GGG$ sequences as the sum of G4 units suitably flanked by TTA sequences (Fig. 3A), it is notable that they are not equivalent in terms of G4 units composing them. $(GGGTTA)_3GGG$ (H21) is an individual G4 without TTA flanking sequences. $(GGGTTA)_7GGG$ (H45) is composed of two different G4 units: one flanked by a TTA tail at its 3′ side (H21-TTA) and one flanked by a TTA tail at its 5′ side (TTA-H21). $(GGGTTA)_{11}GGG$ (H69) is composed of three different G4 units: the two terminal G4 units H21-TTA and TTA-H21, and a central G4 unit flanked by a TTA tail at both its sides (TTA-H21-TTA). And so forth: a $(GGGTTA)_{4m-1}GGG$ tandem G4 structure (where $m = 2, 3, 4, \ldots$ corresponds to the number of G4 units) is composed of the two terminal G4 units H21-TTA and TTA-H21, and of $m - 2$ central G4 units TTA-H21-TTA. It is known that flanking nucleotides affect the conformation of the G4 formed by the H21-core sequence (for review [37]); they may also affect its stability [22,38]. We hence wondered if the global stability of tandem G4 structures may be explained solely in terms of the impact of TTA flanking tails on the single G4 units composing them. To answer to this question, we first investigated the influence of TTA tails on the stability of an individual telomeric G4 and we verified if the tandem G4 structures formed by $(GGGTTA)_{7,11,15}GGG$ sequences are equivalent to the sum of non-linked single G4 units, suitably flanked by TTA tails as represented in Fig. 3A.

3.2. Influence of TTA tails on the stability of an individual telomeric G4 and comparison of $(GGGTTA)_{7,11,15}GGG$ structures with the sum of non-linked G4 units

We studied the impact of TTA tails on the stability of the G4 structure formed by the H21-core sequence. Three sequences were studied: H21-TTA, mimicking a G4 unit at the 5′ end of a $(GGGTTA)_{4m-1}GGG$ tandem structure; TTA-H21-TTA, mimicking an inner G4 unit in a tandem context; and TTA-H21, mimicking a G4 unit at the 3′ end of a $(GGGTTA)_{4m-1}GGG$ tandem structure, as represented in Fig. 3A (sequences are reported in Table 1). In all cases, the TTA flanking tails destabilized the G4 structure, but the extent of destabilization depended on their position: H21-TTA was more stable than TTA-H21 (65 °C vs 60 °C), while TTA tails at both sides (TTA-H21-TTA) destabilized to the larger extent (55 °C) (Fig. 4A). Likely a TTA tail, depending on its position (5′ side, 3′ side or both sides), drives the folding of the whole sequence into different G4 conformations characterized by different stabilities, as suggested by nuclear magnetic resonance (NMR) studies on TA-H21, H21-T(T) and (T)TA-H21-TT sequences [17,19–22,32].

Table 1
Studied sequences, melting temperatures at 295 nm and Gibbs free energy changes upon folding at 37 °C, in the presence of 100 mM KCl.

Sequence name	Sequence (from 5′ to 3′)	Number of potential G4 units	T_m (°C)	ΔG^0 (310 K) (kcal mol^{-1})
H21	$(GGGTTA)_3GGG$	1	68	
H45	$(GGGTTA)_7GGG$	2	59	
H69	$(GGGTTA)_{11}GGG$	3	56	
H93	$(GGGTTA)_{15}GGG$	4	54	
H21-TTA	$(GGGTTA)_3GGGTTA$	1	65	−5.6
TTA-H21-TTA	$TTA(GGGTTA)_3GGGTTA$	1	55	−3.2
TTA-H21	$TTA(GGGTTA)_3GGG$	1	60	−3.5
H51	$TTA(GGGTTA)_7GGGTTA$	2	50	
H75	$TTA(GGGTTA)_{11}GGGTTA$	3	50	
H99	$TTA(GGGTTA)_{15}GGGTTA$	4	50	
H45-TTA	$(GGGTTA)_7GGGTTA$	2	57	
TTA-H45	$TTA(GGGTTA)_7GGG$	2	55	
H21-$(TTA)_2$-H21	$(GGGTTA)_3GGG\ (TTA)_2(GGGTTA)_3GGG$	2	58	
H21-$(TTA)_3$-H21	$(GGGTTA)_3GGG\ (TTA)_3(GGGTTA)_3GGG$	2	58	

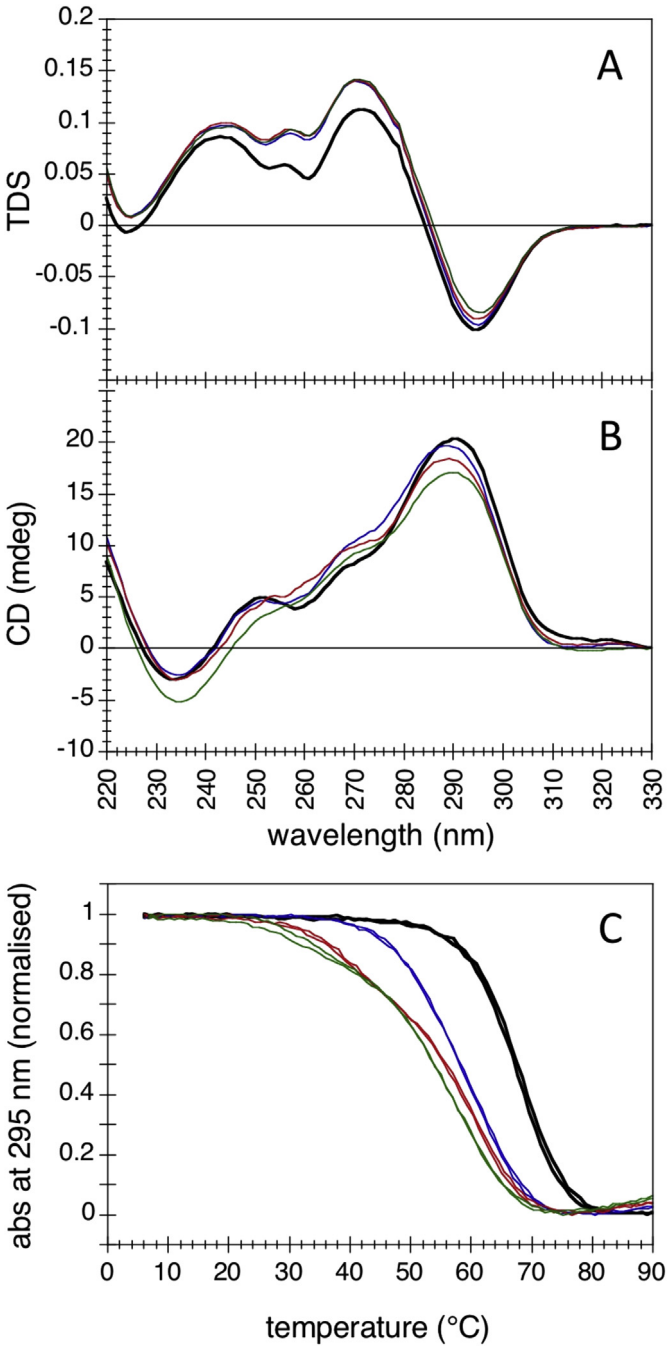

Fig. 1. Structure and stability of $(GGGTTA)_{n=3,7,11,15}GGG$ oligonucleotides. (A) TDS, (B) CD spectra at 5 °C, (C) melting profiles at 295 nm (normalized between the minimum and the maximum of absorbance) of H21 ($n = 3$, black bold line), H45 ($n = 7$, blue line), H69 ($n = 11$, red line) and H93 ($n = 15$, green line), in 100 mM KCl, at strand concentrations corresponding to 6 μM of potential G4 units (H21: 6 μM, H45: 3 μM, H69: 2 μM, H93: 1.5 μM).

The impact of TTA tails on the stability of an individual G4 suggests that, in the G4 tandem structures formed by $(GGGTTA)_{4m-1}GGG$ sequences ($m = 2, 3, 4, \ldots$), the 5′ terminal G4 (mimicked by H21-TTA) has a higher stability than the 3′ terminal G4 (mimicked by TTA-H21), while the inner G4 units (mimicked by TTA-H21-TTA) have the lowest stability (Fig. 3A). This explains the decrease in melting temperature with increasing the number of G4 units for $(GGGTTA)_{3,7,11,15}GGG$ oligonucleotides. $(GGGTTA)_7GGG$ (H45) is less stable than $(GGGTTA)_3GGG$ (H21) because it is

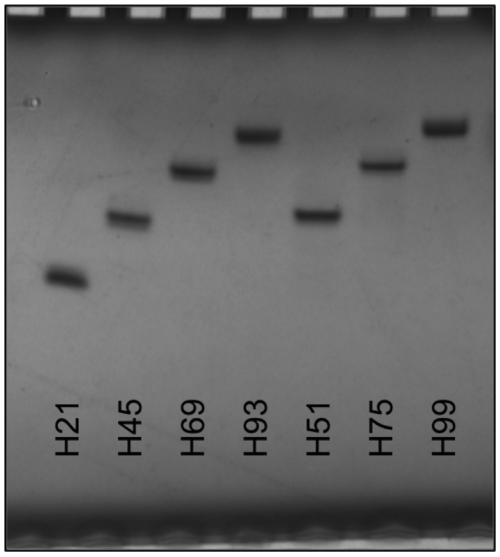

Fig. 2. Non-denaturing PAGE of $(GGGTTA)_{3,7,11,15}GGG$ and TTA-$(GGGTTA)_{7,11,15}GGG$-TTA oligonucleotides. Migration pattern of H21, H45, H69, H93 and of H51, H75, H99 in KCl, at strand concentrations corresponding to 60 μM of potential G4 units (H21: 60 μM, H45 and H51: 30 μM, H69 and H75: 20 μM, H93 and H99: 15 μM).

composed of two G4 units (H21-TTA and TTA-H21), which have both a lower stability (65 °C and 60 °C) than $(GGGTTA)_3GGG$ (H21) (68 °C). $(GGGTTA)_{11}GGG$ (H69) is less stable than $(GGGTTA)_7GGG$ (H45) because, in addition to the two terminal G4 units H21-TTA and TTA-H21, it bears an inner G4 unit (TTA-H21-TTA) of lower stability (55 °C). Finally $(GGGTTA)_{15}GGG$ (H93) is less stable than $(GGGTTA)_{11}GGG$ (H69) because it bears an additional central unit (TTA-H21-TTA) of low stability. This effect can be observed in the melting profiles of mixtures of G4 monomers representing H45, H69 and H93 tandem structures: the T_m of the mix H21-TTA + TTA-H21 (representing H45) is higher than the T_m of the mix H21-TTA + TTA-H21-TTA + TTA-H21 (representing H69), which, in turn, is higher than the T_m of the mix H21-TTA + 2x(TTA-H21-TTA) + TTA-H21 (representing H93) (Fig. 4B).

In conclusion, the impact of TTA flanking tails on the stability of a single G4-core qualitatively accounts for the decrease in thermal stability with increasing number of G4 units for structures formed by $(GGGTTA)_{3,7,11,15}GGG$ sequences. To further verify this hypothesis, we studied TTA-$(GGGTTA)_{7,11,15}GGG$-TTA sequences.

3.3. Formation and stability of tandem G4 by TTA-$(GGGTTA)_{7,11,15}GGG$-TTA sequences

Unlike $(GGGTTA)_{4m-1}GGG$ sequences, TTA-$(GGGTTA)_{4m-1}GGG$-TTA sequences are composed of potential G4 units that are identical in term of flanking sequences. Indeed each G4 unit, inner as well as terminal, is flanked by a TTA tail at both its 5′ and 3′ sides, as represented in Fig. 3B. Hence, if a G4 unit in a tandem context is affected by and only by its flanking TTA tails, then the structures formed by TTA-$(GGGTTA)_{4m-1}GGG$-TTA sequences should display similar melting profiles, unlike $(GGGTTA)_{4m-1}GGG$ sequences. To ascertain this assumption, we studied the following sequences: TTA-$(GGGTTA)_{7,11,15}GGG$-TTA (named H51, H75 and H99, respectively, as reported in Table 1).

First, we ascertained by TDS and CD that TTA-$(GGGTTA)_{7,11,15}GGG$-TTA sequences (i.e. H51, H75 and H99) folded into contiguous G4s, as done for $(GGGTTA)_{7,11,15}GGG$ sequences. The TDS and CD spectra of H51, H75 and H99 at 3, 2 and 1.5 μM strand concentration, respectively, were identical in shape and intensity to

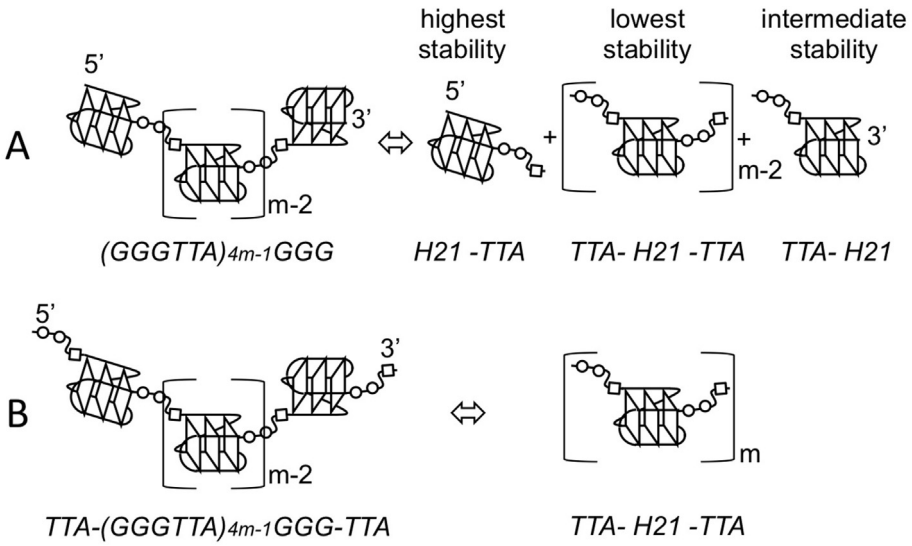

Fig. 3. Representation of tandem G4 structures as the sum of non-linked G4 monomers. (A) $(GGGTTA)_{4m-1}GGG$ structures are composed of a G4 unit flanked by a TTA tail at its 3′ side (H21-TTA), $m - 2$ G4 units flanked by TTA tails at both sides (TTA-H21-TTA) and a G4 unit flanked by a TTA tail at its 5′ side (TTA-H21). (B) TTA-$(GGGTTA)_{4m-1}GGG$-TTA structures are composed of m G4 units flanked by TTA tails at both sides (TTA-H21-TTA). The symbols ○○□ represent TTA tails.

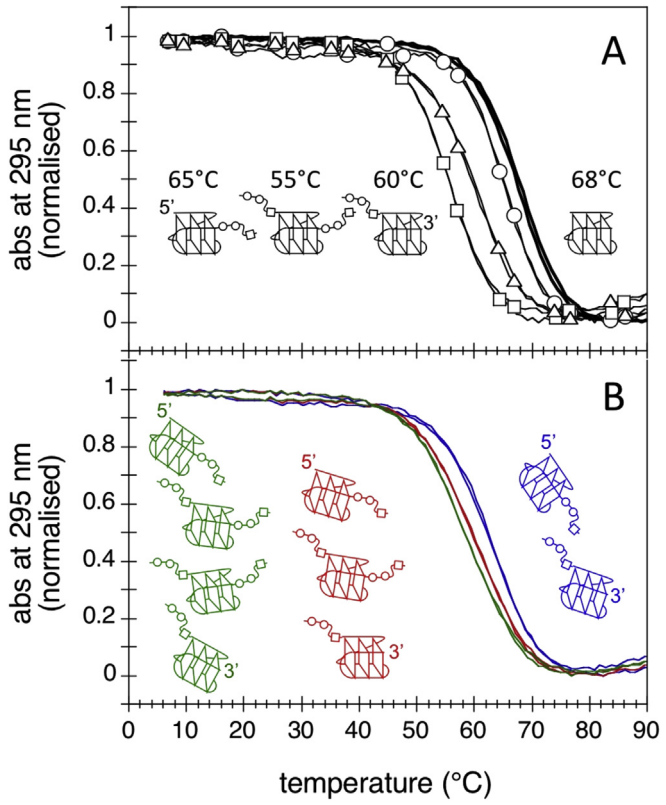

Fig. 4. Melting profiles of G4 monomers and of mixes of G4 monomers. (A) Melting profiles at 295 nm (normalized between the minimum and the maximum of absorbance) of H21 (bold line), H21-TTA (circles), TTA-H21-TTA (squares) and TTA-H21 (triangles), in 100 mM KCl, at 3 μM strand concentration. Schematic representation of the three G4 monomers and their T_m values; the symbols ○○□ represent TTA tails. (B) Melting profiles at 295 nm (normalized between the minimum and the maximum of absorbance) of mixes of G4 monomers, in 100 mM KCl. Blue line: H21-TTA + TTA-H21 (representing H45); red line: H21-TTA + TTA-H21-TTA + TTA-H21 (representing H69); green line: H21-TTA + twofold TTA-H21-TTA + TTA-H21 (representing H93). Schematic representation of the three mixes of monomers.

the ones of H21 at 6 μM strand concentration (Fig. 5A and B). This proves that H51, H75 and H99 fold into two, three and four contiguous G4s, respectively. The non-denaturing PAGE migration pattern further supports folding of each of the three oligonucleotides H51, H75 and H99 into a single stable conformer (Fig. 2). Unlike H45, H69 and H93 sequences, the structures formed by H51, H75 and H99 displayed identical melting temperatures (50 °C) (Fig. 5C). This supports that, unlike $(GGGTTA)_{7,11,15}GGG$ structures, TTA-$(GGGTTA)_{7,11,15}GGG$-TTA tandem G4 structures are composed of G4 units of similar stabilities.

Overall, our data on $(GGGTTA)_{3,7,11,15}GGG$ and TTA-$(GGGTTA)_{3,7,11,15}GGG$-TTA sequences further support that the stability of a G4 unit in a tandem context is mainly affected by its TTA flanking tails. This explains why the T_m of $(GGGTTA)_{7,11,15}GGG$ structures decreases upon increasing the number of G4 units, whereas the T_m of TTA-$(GGGTTA)_{7,11,15}GGG$-TTA structures is independent of the number of G4 units.

3.4. Influence of the length of the linker connecting two G4 units on the stability of a tandem structure

In order to confirm that the trinucleotide TTA flanking sequences are the major determinants of the stability of a G4 unit in a tandem context, we studied the following sequences: H21-$(TTA)_n$-H21 where $n = 1, 2, 3$ (Table 1). These sequences fold into two contiguous G4 units, separated by one ($n = 1$), two ($n = 2$) or three ($n = 3$) TTA repeats (for $n = 1$, the sequence is the telomeric sequence H45). The global stability of the tandem G4 structures formed by these sequences did not depend on the number of TTA repeats separating two adjacent G4 units (Fig. 6). This suggests that the G4 units are independent and further supports that they are mainly affected by their adjacent TTA tails.

3.5. Probing the impact of TTA tails on the terminal G4 units in a tandem context

The study of the monomeric G4s formed by H21-TTA, TTA-H21-TTA and TTA-H21 sequences allowed us indirectly inferring the relative stability of G4 units in a tandem context according to their position. To directly probe the impact of TTA tails on the two

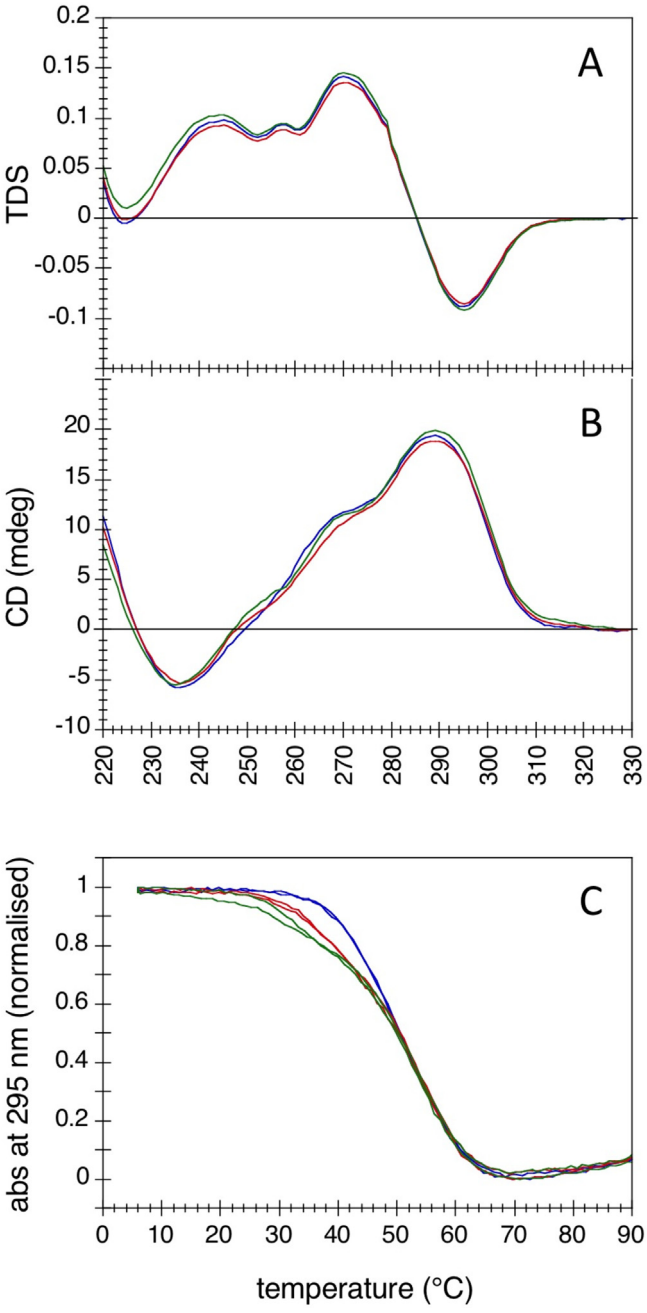

Fig. 5. Structure and stability of TTA-$(GGGTTA)_{n=7,11,15}$GGG-TTA oligonucleotides. (A) TDS, (B) CD spectra at 5 °C, (C) melting profiles at 295 nm (normalized between the minimum and the maximum of absorbance) of H51 (n = 7, blue line), H75 (n = 11, red line) and H99 (n = 15, green line), in 100 mM KCl, at strand concentrations corresponding to 6 μM of potential G4 units (H51: 3 μM, H75: 2 μM, H99: 1.5 μM).

terminal G4 units in a tandem context (the one at the 5′ end and the one at the 3′ end), we studied the following sequences TTA-H45 and H45-TTA (Table 1). The tandem structure formed by TTA-H45 is composed of a 5′ terminal G4 flanked by a TTA tail and of a blunt 3′ terminal G4; the tandem structure formed by H45-TTA is composed of a blunt 5′ terminal G4 and of a 3′ terminal G4 flanked by a TTA tail. The T_m values of TTA-H45 and H45-TTA were 55 and 57 °C, respectively; they were lower than the T_m of H45 (59 °C), i.e. the structure composed of two blunt terminal G4s (Fig. 7). In agreement with results obtained on monomeric G4s, these data demonstrate that also in a tandem context (*i*) a terminal G4 units

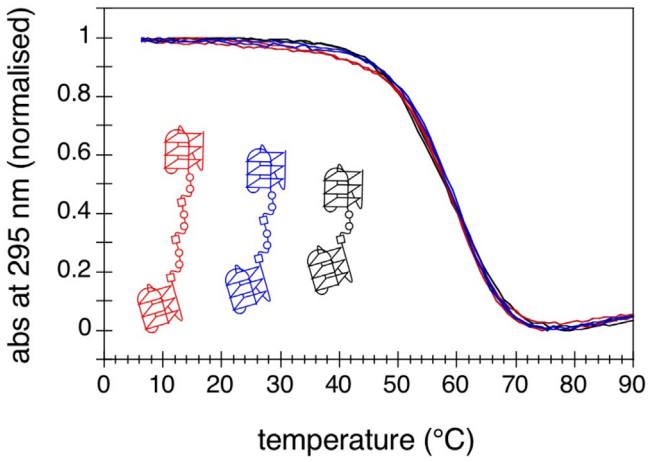

Fig. 6. Melting curves of H21-$(TTA)_n$-H21 oligonucleotides. Melting profiles at 295 nm (normalized between the minimum and the maximum of absorbance) of H21-$(TTA)_n$-H21 sequences (n = 1: black line, n = 2: blue line, n = 3: red line), at 3 μM strand concentrations, in 100 mM KCl. Schematic representation of the three structures; the symbols ○ ○□ represent TTA tails.

(5′ or 3′) is destabilized by the presence of a flanking TTA tail; (*ii*) a TTA tail at the 5′ terminal G4 unit destabilizes the G4-core to a larger extent than a TTA tail at the 3′ terminal G4 unit, in other words that the stability of the 3′ terminal G4 unit is less affected by a TTA flanking tail than the stability of the 5′ terminal G4 unit.

4. Discussion

In the past ten years, a few studies have addressed the question of the stability of structures formed by long telomeric strands. Some lines of evidence of spontaneous folding into contiguous G4 have been provided. Nevertheless, the published data (mainly limited to two and three potential contiguous G4) do not yet allow drawing a clear picture of the stability of these higher-order structures and no study has provided an interpretation of the observed stabilities of these structures. The aim of this study was to provide (*i*) a clarified picture of the stability of telomeric tandem G4 structures as a function of the number of G4 units and of boundary

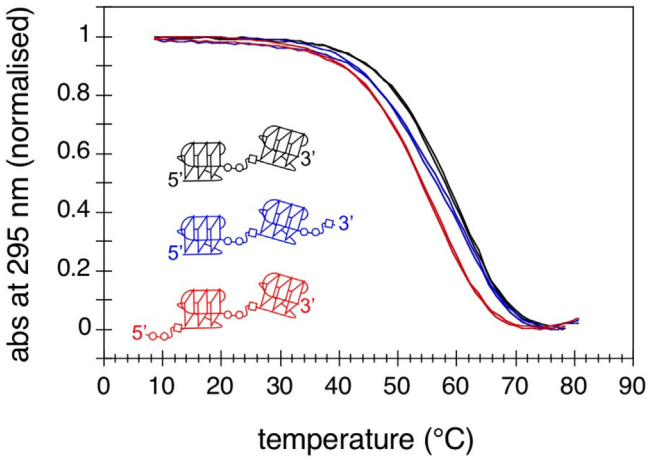

Fig. 7. Melting curves of TTA-H45, H45-TTA and H45 oligonucleotides. Melting profiles at 295 nm (normalized between the minimum and the maximum of absorbance) of TTA-H45 (red), H45-TTA (blue) and H45 (black) sequences, at 3 μM strand concentrations, in 100 mM KCl. Schematic representation of the three structures; the symbols ○ ○□ represent TTA tails.

sequences and (*ii*) an understanding of the diversity of their melting behaviors in terms of the single G4 units composing them.

We proved that both types of sequences, $(GGGTTA)_{n=7,11,15}GGG$ and TTA-$(GGGTTA)_{n=7,11,15}$GGG-TTA, fold into tandem G4s, thus providing, for the first time, spectroscopic evidence of folding of telomeric strands into up to four contiguous G4s. We showed that the melting temperature of $(GGGTTA)_{7,11,15}GGG$ tandem structures decreases upon increasing the number of G4 units (59, 56 and 54 °C, respectively), while the melting temperature of TTA-$(GGGTTA)_{7,11,15}$GGG-TTA tandem structures is independent of the number of G4 units (50 °C).

To explain the reasons of these different behaviors, we represented telomeric tandem G4 structures as the sum of G4 units suitable flanked by TTA tails (as shown in Fig. 3). TTA-$(GGGTTA)_{4m-1}$GGG-TTA structures are composed of m G4 units, which are identical in terms of flanking sequences (all of them, the two terminal G4s as well as the inner G4s, are flanked by TTA tails at both their sides). $(GGGTTA)_{4m-1}GGG$ structures are composed of three types of G4 units of different stabilities: a 5′ terminal G4 (mimicked by H21-TTA, displaying the highest stability), $m - 2$ inner G4 units (mimicked by TTA-H21-TTA, displaying the lowest stability), and a 3′ terminal G4 (mimicked by TTA-H21, displaying an intermediate stability). This explains why, in contrast to TTA-$(GGGTTA)_{7,11,15}$GGG-TTA, the stability of $(GGGTTA)_{7,11,15}GGG$ structures decreases with increasing number of G4 units (two, three and four). A reasonable prediction is that, if the G4 units are independent (as suggested by our results on the impact of $(TTA)_n$ linkers on the stability of a tandem structure), then, upon further increasing the number of G4 units, the stability of $(GGGTTA)_{4m-1}GGG$ structures should not decrease indefinitely, but should approach the stability of an inner G4 unit. This reasonable hypothesis is difficult to prove experimentally, because of the difficulty to synthetize and accurately characterize sequences bearing more than a few G4 units.

Our conclusions about the relative stabilities of the G4 units as a function of their position in $(GGGTTA)_{4m-1}GGG$ structures were drawn from results obtained with individual G4s (H21-TTA, TTA-H21-TTA and TTA-H21), and they were supported by results obtained with dimeric G4s (H45, H45-TTA and TTA-H45). We also carried out melting experiments followed by fluorescence on the three G4 units of the H69 sequence individually labeled with a fluorescein and a tetramethylrhodamine. The double-dye labeled inner G4 unit displayed the lowest thermal stability, while the double-dye labeled 5′ and 3′ terminal G4 units displayed higher stabilities (Fig. S1). Nevertheless, results obtained with labeled G4 units must be interpreted with caution: labeling affects the stability of a G4, so that information obtained on labeled units cannot be directly transposed to unlabeled units.

A rough estimation of the stabilities of a G4 unit in a $(GGGTTA)_{4m-1}GGG$ tandem context when moving from the 5′ toward the 3′ end along the strand is provided by Gibbs free energy changes (ΔG^0) extrapolated from an analysis of melting transitions of H21-TTA, TTA-H21-TTA and H21-TTA sequences (Table 1). For these three sequences, fitting according to a two-state model was satisfactory (Fig. S2). This is consistent with what reported by Petraccone et al. for a similar sequence (TTA-H21-TT), for which analysis of melting revealed negligible intermediate species [30]. H21-TTA (mimicking the G4 unit at the 5′ end of $(GGGTTA)_{4m-1}GGG$ structures) is significantly more stable than TTA-H21-TTA (mimicking an inner G4 unit) (ΔG^0 (37 °C) of −5.6 and −3.2 kcal mol^{-1}, respectively). In contrast, TTA-H21 (mimicking the G4 unit at the 3′ end of $(GGGTTA)_{4m-1}GGG$ structures) has a ΔG^0 (37 °C) of −3.5 kcal mol^{-1}, just slightly more stable than TTA-H21-TTA.

Importantly, this rough estimation of Gibbs free energy changes also suggests that the stability of a G4 unit at the 3′ end of a telomeric strand is not strongly affected by the presence of terminal nucleotides. These conclusions about the effect of TTA flanking tails on the 5′ and 3′ terminal G4 units in a tandem context were also supported by the differences in stabilities displayed by H45, H45-TTA and TTA-H45 structures. Our results explain some data reported by Petraccone et al. [30]: why adding a TT tail at the 3′ extremity of two and three tandem structures formed by $(TTAGGG)_{8,12}$ sequences has not a strong impact on the global stability of the formed structures.

Overall, our results support that telomeric tandem G4 structures are composed, to a good approximation, of independent G4 units and that the stability of each G4 unit in a tandem context is mainly affected by its adjacent TTA tails. Nevertheless, telomeric tandem G4s are not perfectly equivalent to the sum of non-linked G4 units: compared to the tandem structures formed by $(GGGTTA)_{7,11,15}GGG$ sequences, the melting profiles of mixes of non-linked G4s were shifted by 3–4 °C toward higher temperatures; similarly, the TTA-H21-TTA G4 has a higher thermal stability (T_m = 55 °C) than the global structures formed by TTA-$(GGGTTA)_{7,11,15}$GGG-TTA sequences (T_m = 50 °C). According to NMR published studies, flanking nucleotides drive the folding of the H21-core sequence into different conformations, depending on their position (5′-side, 3′-side or both sides), by establishing stabilizing interactions with the G4-core [17,19–22]. Likely, in a tandem context, these stabilizing interactions may be impaired, since each TTA linker is shared by two adjacent G4s. This in turn may affect the conformation and the stability of the G4 units when switching from a single G4 unit to a G4 unit in a tandem context. In other words, “free” TTA tails are not equivalent to “shared” TTA tails, with respect to the possibilities of stabilizing interactions with a G4-core.

This impact of free or shared TTA tails on the stability of a G4-core may also explain why, despite identical thermal stabilities, the melting profiles of TTA-$(GGGTTA)_{n=7,11,15}$GGG-TTA structures are not strictly identical at temperatures below T_m (Fig. 5C). To a first approximation, we proposed that TTA-$(GGGTTA)_{7,11,15}$GGG-TTA tandem structures are composed of non-interacting G4 units of identical stabilities; if this were the case, their melting profiles would be identical. Nevertheless, at temperatures below T_m, the fraction f of folded G4 units decreases upon increasing the length of the sequence (as it can be directly assessed from Fig. 5C). For example, at 37 °C, f decreases from 0.96 to 0.87 to 0.83 upon increasing the number of G4 units from 2 (n = 7) to 3 (n = 11) to 4 (n = 15), respectively. It is noteworthy that the difference in the fraction of folded G4 units between the dimeric and the trimeric structure (f = 0.96 and f = 0.87, respectively) is greater than the one between the trimeric and the tetrameric structure (f = 0.87 and f = 0.83, respectively). This behavior may be explained by a slightly higher stability of the two terminal G4 units compared to inner G4 units. Indeed the tandem structure formed by TTA-$(GGGTTA)_{4m-1}$-TTA sequence (m = 2, 3, …) is composed of a 5′ terminal G4 unit, $m - 2$ internal G4 units and a 3′ terminal G4 unit. If the G4 units are independent, then the folded fraction f of G4 units at a given temperature is given by:

$$f = [f(5'Q) + (m-2)f(iQ) + f(3'Q)]/m.$$

where $f(5'Q)$ is the folded fraction of the 5′ terminal G4 unit, $f(iQ)$ is the folded fraction of an internal G4 unit and $f(3'Q)$ is the folded fraction of the 3′ terminal G4 unit. The difference between the folded fraction of the G4 units of a structure composed of m units (f_m) and the folded fraction of G4 units of a structure composed of $m + 1$ units (f_{m+1}) is then:

$$f_m - f_{m+1} = [f(5'Q) - 2f(iQ) + f(3'Q)]/[m(m+1)].$$

If the stabilities of the 5′ and 3′ terminal G4 units are higher than the stability of an internal G4 unit then this difference is positive and decreases with increasing *m*. This is what observed for TTA-$(GGGTTA)_{7,11,15}$GGG-TTA structures. Likely, compared to inner G4 units, the conformations of the two terminal G4 units may be slightly stabilized by favorable interactions with their free TTA flanking tails.

From a biological standpoint, our study provides information about the global and local stability of tandem G4 structures at the 3′-overhangs of human telomeres. Concerning the global stability, for the longer telomeric sequence we studied (99 nucleotides), we estimated, by analysis of melting profiles, that, under nearly physiological salt and temperature conditions (100 mM KCl, 37 °C), about 80% of the potential G4 units are folded. Concerning the local stability, our study provides interesting information about the relative stability of the very last G4 unit, the one formed at the very 3′ end of a telomeric overhang. In human cells, the termination of the telomeric 3′-overhang is variable, with a preference for $TTAG^{3'}$, $TTA^{3'}$ and $TT^{3'}$ terminations [39]. Our results on the impact of flanking tails on the stability of the G4-core formed by H21 strongly suggest that, under nearly physiological conditions, the terminal G4 unit at the very 3′ end of a telomeric overhang should be roughly as stable as an inner G4, disregarding the 3′ termination (at 37 °C, TTA-H21 and TTA-H21-TTA G4s have similar stabilities). This implies that proteins binding to telomeric overhangs have to deal with structural G4 units of similar stabilities, disregarding the 3′ termination of the telomeric overhang. It is noteworthy that if telomeres ended with a 5′- (instead of a 3′-) overhang, this would not be the case: the very last G4 on a hypothetical 5′-overhang ending with $GGG^{5'}$ would be much more stable that the inner G4s (at 37 °C, H21-TTA is more stable than TTA-H21-TTA).

The biological role of tandem G4 at telomeres, in particular at the 3′-overhang still remains elusive. The telomeric 3′-overhang participates in capping and regulation of telomeres. Folding of a transiently exposed telomeric 3′-overhang into tandem G4s might provide protection from binding of non-shelterin proteins or modulate their binding, as suggested by recent *in vitro* studies [14,15]. G4s at human telomeric 3′-overhang might have a capping function, when normal capping is impaired, as it has been suggested in a budding yeast [6]. Are G4s at telomeres functional or just challenging structures? May be both. What is evident is that evolution has preserved the potential of human telomeric sequences, and, in particular, of the telomeric 3′-overhang to fold into tandem G4s.

5. Conclusions

In conclusion, our study provides an explication of the stability of telomeric tandem G4 structures as a function of the number of G4 units and of boundary sequences. (*i*) We explain, in terms of the single G4 units composing the tandem structures, why the stability of $(GGGTTA)_{4m-1}$GGG structures decreases with increasing number of G4 units, whereas the stability of TTA-$(GGGTTA)_{4m-1}$GGG-TTA structures does not. (*ii*) We provide an explanation of the stability of a G4 unit in a tandem context. Our work supports that the inner G4 units have similar stabilities, whereas the stabilities of the terminal G4 units are modulated by their flanking nucleotides: in a TTA-$(GGGTTA)_{4m-1}$GGG-TTA tandem context, the terminal G4 units are roughly as stable as the inner G4 units; while in a $(GGGTTA)_{4m-1}$GGG tandem context, the G4 at the 5′ extremity is more stable than the G4 at the 3′ extremity, which in turn in more stable than an inner G4.

Author contributions

P. A. designed the research and performed most of the experiments; A. B. contributed to the design and execution of experiments. P. A. wrote the manuscript; A.B. critical read it.

Conflict of interest statement

No conflict of interest.

Acknowledgments

We thank Dr. Carole Saintomé and Dr. Anne De Cian for critical reading the manuscript. This work was financially supported by Muséum National d'Histoire Naturelle (MNHN), Centre National de la Recherche Scientifique (CNRS), Institut National de la Santé et de la Recherche Médicale (INSERM).

Appendix A. Supplementary material

Supplementary data related to this article can be found online at http://dx.doi.org/10.1016/j.biochi.2015.04.003.

References

[1] T. de Lange, How telomeres solve the end-protection problem, Science 326 (2009) 948–952.
[2] R.J. O'Sullivan, J. Karlseder, Telomeres: protecting chromosomes against genome instability, Nat. Rev. Mol. Cell Biol. 11 (2010) 171–181.
[3] R.J. Wellinger, D. Sen, The DNA structures at the ends of eukaryotic chromosomes, Eur. J. Cancer 33 (1997) 735–749.
[4] P.L. Tran, J.L. Mergny, P. Alberti, Stability of telomeric G-quadruplexes, Nucl. Acids Res. 39 (2011) 3282–3294.
[5] H.J. Lipps, D. Rhodes, G-quadruplex structures: in vivo evidence and function, Trends Cell Biol. 19 (2009) 414–422.
[6] J.S. Smith, Q. Chen, L.A. Yatsunyk, J.M. Nicoludis, M.S. Garcia, R. Kranaster, S. Balasubramanian, D. Monchaud, M.P. Teulade-Fichou, L. Abramowitz, et al., Rudimentary G-quadruplex-based telomere capping in *Saccharomyces cerevisiae*, Nat. Struct. Mol. Biol. 18 (2011) 478–485.
[7] L. Crabbe, R.E. Verdun, C.I. Haggblom, J. Karlseder, Defective telomere lagging strand synthesis in cells lacking WRN helicase activity, Science 306 (2004) 1951–1953.
[8] A. Sfeir, S.T. Kosiyatrakul, D. Hockemeyer, S.L. MacRae, J. Karlseder, C.L. Schildkraut, T. de Lange, Mammalian telomeres resemble fragile sites and require TRF1 for efficient replication, Cell 138 (2009) 90–103.
[9] J.B. Vannier, V. Pavicic-Kaltenbrunner, M.I. Petalcorin, H. Ding, S.J. Boulton, RTEL1 dismantles T loops and counteracts telomeric G4-DNA to maintain telomere integrity, Cell 149 (2012) 795–806.
[10] D. Gomez, R. Paterski, T. Lemarteleur, K. Shin-Ya, J.L. Mergny, J.F. Riou, Interaction of telomestatin with the telomeric single-strand overhang, J. Biol. Chem. 279 (2004) 41487–41494.
[11] A.M. Zahler, J.R. Williamson, T.R. Cech, D.M. Prescott, Inhibition of telomerase by G-quartet DNA structures, Nature 350 (1991) 718–720.
[12] T.M. Fletcher, D. Sun, M. Salazar, L.H. Hurley, Effect of DNA secondary structure on human telomerase activity, Biochemistry 37 (1998) 5536–5541.
[13] L. Oganesian, I.K. Moon, T.M. Bryan, M.B. Jarstfer, Extension of G-quadruplex DNA by ciliate telomerase, EMBO J. 25 (2006) 1148–1159.
[14] S. Ray, J.N. Bandaria, M.H. Qureshi, A. Yildiz, H. Balci, G-quadruplex formation in telomeres enhances POT1/TPP1 protection against RPA binding, Proc. Natl. Acad. Sci. U. S. A. 111 (2014) 2990–2995.
[15] H. Hwang, A. Kreig, J. Calvert, J. Lormand, Y. Kwon, J.M. Daley, P. Sung, P.L. Opresko, S. Myong, Telomeric overhang length determines structural dynamics and accessibility to telomerase and ALT-associated proteins, Structure 22 (2014) 842–853.
[16] Y. Xu, Y. Noguchi, H. Sugiyama, The new models of the human telomere d [AGGG(TTAGGG)3] in K+ solution, Bioorg. Med. Chem. 14 (2006) 5584–5591.
[17] K.N. Luu, A.T. Phan, V. Kuryavyi, L. Lacroix, D.J. Patel, Structure of the human telomere in K+ solution: an intramolecular (3+1) G-quadruplex scaffold, J. Am. Chem. Soc. 128 (2006) 9963–9970.
[18] A. Ambrus, D. Chen, J. Dai, T. Bialis, R.A. Jones, D. Yang, Human telomeric sequence forms a hybrid-type intramolecular G-quadruplex structure with mixed parallel/antiparallel strands in potassium solution, Nucl. Acids Res. 34 (2006) 2723–2735.
[19] A.T. Phan, K.N. Luu, D.J. Patel, Different loop arrangements of intramolecular human telomeric (3+1) G-quadruplexes in K+ solution, Nucl. Acids Res. 34 (2006) 5715–5719.

[20] J. Dai, M. Carver, C. Punchihewa, R.A. Jones, D. Yang, Structure of the hybrid-2 type intramolecular human telomeric G-quadruplex in K+ solution: insights into structure polymorphism of the human telomeric sequence, Nucl. Acids Res. 35 (2007) 4927–4940.
[21] A.T. Phan, V. Kuryavyi, K.N. Luu, D.J. Patel, Structure of two intramolecular G-quadruplexes formed by natural human telomere sequences in K+ solution, Nucl. Acids Res. 35 (2007) 6517–6525.
[22] K.W. Lim, S. Amrane, S. Bouaziz, W. Xu, Y. Mu, D.J. Patel, K.N. Luu, A.T. Phan, Structure of the human telomere in K+ solution: a stable basket-type G-quadruplex with only two G-tetrad layers, J. Am. Chem. Soc. 131 (2009) 4301–4309.
[23] K.W. Lim, V.C. Ng, N. Martin-Pintado, B. Heddi, A.T. Phan, Structure of the human telomere in Na+ solution: an antiparallel (2+2) G-quadruplex scaffold reveals additional diversity, Nucl. Acids Res. 41 (2013) 10556–10562.
[24] V.L. Makarov, Y. Hirose, J.P. Langmore, Long G tails at both ends of human chromosomes suggest a C strand degradation mechanism for telomere shortening, Cell 88 (1997) 657–666.
[25] W.E. Wright, V.M. Tesmer, K.E. Huffman, S.D. Levene, J.W. Shay, Normal human chromosomes have long G-rich telomeric overhangs at one end, Genes Develop. 11 (1997) 2801–2809.
[26] A. Cummaro, I. Fotticchia, M. Franceschin, C. Giancola, L. Petraccone, Binding properties of human telomeric quadruplex multimers: a new route for drug design, Biochimie 93 (2011) 1392–1400.
[27] X.X. Huang, L.N. Zhu, B. Wu, Y.F. Huo, N.N. Duan, D.M. Kong, Two cationic porphyrin isomers showing different multimeric G-quadruplex recognition specificity against monomeric G-quadruplexes, Nucl. Acids Res. 42 (2014) 8719–8731.
[28] H.Q. Yu, D. Miyoshi, N. Sugimoto, Characterization of structure and stability of long telomeric DNA G-quadruplexes, J. Am. Chem. Soc. 128 (2006) 15461–15468.
[29] Y. Xu, T. Ishizuka, K. Kurabayashi, M. Komiyama, Consecutive formation of G-quadruplexes in human telomeric-overhang DNA: a protective capping structure for telomere ends, Angew. Chemie 48 (2009) 7833–7836.
[30] L. Petraccone, C. Spink, J.O. Trent, N.C. Garbett, C.S. Mekmaysy, C. Giancola, J.B. Chaires, Structure and stability of higher-order human telomeric quadruplexes, J. Am. Chem. Soc. 133 (2011) 20951–20961.
[31] V. Singh, M. Azarkh, M. Drescher, J.S. Hartig, Conformations of individual quadruplex units studied in the context of extended human telomeric DNA, Chem. Commun. 48 (2012) 8258–8260.
[32] R. Hansel, F. Lohr, L. Trantirek, V. Dotsch, High-resolution insight into G-overhang architecture, J. Am. Chem. Soc. 135 (2013) 2816–2824.
[33] M. Vorlickova, J. Chladkova, I. Kejnovska, M. Fialova, J. Kypr, Guanine tetraplex topology of human telomere DNA is governed by the number of (TTAGGG) repeats, Nucl. Acids Res. 33 (2005) 5851–5860.
[34] L. Bauer, K. Tluckova, P. Tohova, V. Viglasky, G-quadruplex motifs arranged in tandem occurring in telomeric repeats and the insulin-linked polymorphic region, Biochemistry 50 (2011) 7484–7492.
[35] J.L. Mergny, J. Li, L. Lacroix, S. Amrane, J.B. Chaires, Thermal difference spectra: a specific signature for nucleic acid structures, Nucl. Acids Res. 33 (2005) e138.
[36] J.L. Mergny, L. Lacroix, Analysis of thermal melting curves, Oligonucleotides 13 (2003) 515–537.
[37] A.T. Phan, Human telomeric G-quadruplex: structures of DNA and RNA sequences, FEBS J. 277 (2010) 1107–1117.
[38] V. Viglasky, L. Bauer, K. Tluckova, P. Javorsky, Evaluation of human telomeric g-quadruplexes: the influence of overhanging sequences on quadruplex stability and folding, J. Nucl. Acids 2010 (2010).
[39] A.J. Sfeir, W. Chai, J.W. Shay, W.E. Wright, Telomere-end processing the terminal nucleotides of human chromosomes, Mol. Cell 18 (2005) 131–138.